THE JOURNAL OF BIOLOGICAL CHEMISTRY VOL. 285, NO. 34, pp. 26279–26288, August 20, 2010

Exosome Secretion Ameliorates Lysosomal Storage of Cholesterol in Niemann-Pick Type C Disease*[S]

Received for publication, April 15, 2010, and in revised form, June 15, 2010 Published, JBC Papers in Press, June 16, 2010, DOI 10.1074/jbc.M110.134775

Katrin Strauss[‡§], Cornelia Goebel[¶], Heiko Runz[‖], Wiebke Möbius[**], Sievert Weiss[‡], Ivo Feussner[¶], Mikael Simons[‡‡], and Anja Schneider[‡§1]

From the [‡]Max-Planck-Institute for Experimental Medicine, Hermann-Rein-Strasse 3, Goettingen 37075, Germany, the [§]Department of Psychiatry and Psychotherapy, University Medicine Goettingen, Von-Siebold-Strasse 5, Goettingen 37075, Germany, the [¶]Department for Plant Biochemistry, Albrecht-von-Haller-Institute for Plant Sciences, Georg-August-University, Justus-von-Liebig-Weg 11, Goettingen 37077, Germany, the [‖]Department of Human Genetics, University of Heidelberg, Im Neuenheimer Feld 366, Heidelberg 69120, Germany, the [**]Neurogenetics Department, Max-Planck-Institute for Experimental Medicine, Hermann-Rein-Strasse 3, Goettingen 37075, Germany, and the [‡‡]Department of Neurology, University Medicine Goettingen, Robert-Koch-Strasse 40, Goettingen 37075, Germany

Niemann-Pick type C1 disease is an autosomal-recessive lysosomal storage disorder. Loss of function of the *npc1* gene leads to abnormal accumulation of free cholesterol and sphingolipids within the late endosomal and lysosomal compartments resulting in progressive neurodegeneration and dysmyelination. Here, we show that oligodendroglial cells secrete cholesterol by exosomes when challenged with cholesterol or U18666A, which induces late endosomal cholesterol accumulation. Up-regulation of exosomal cholesterol release was also observed after siRNA-mediated knockdown of NPC1 and in fibroblasts derived from NPC1 patients and could be reversed by expression of wild-type NPC1. We provide evidence that exosomal cholesterol secretion depends on the presence of flotillin. Our findings indicate that exosomal release of cholesterol may serve as a cellular mechanism to partially bypass the traffic block that results in the toxic lysosomal cholesterol accumulation in Niemann-Pick type C1 disease. Furthermore, we suggest that secretion of cholesterol by exosomes contributes to maintain cellular cholesterol homeostasis.

Exosomes are small vesicles of 50–100-nm diameter that are secreted by a variety of cell types. They are generated by inward budding of the late endosomal membrane, which gives rise to intraluminal vesicles within late endosomes. After accumulation of intraluminal vesicles, these compartments are termed multivesicular bodies (MVBs).[2] MVBs can either be routed to lysosomes for degradation or fuse with the plasma membrane to discharge their intraluminal vesicles as exosomes to the extracellular space. The mechanisms that regulate the sorting of proteins to late endosomes and intraluminal vesicles and the segregation between lysosomal degradation and exocytic release are poorly understood, as are the factors that regulate the rate of exosome secretion (1, 2).

Exosomes are involved in numerous processes including cell-cell communication by horizontal transfer of proteins, lipids, and RNA, antigen presentation, tumor metastasis, propagation of infectious agents, and release of superfluous membranes and cytosol (3–7). Reticulocytes utilize exosomes to dispose plasma membrane and cytosol during their maturation to erythrocytes (8). Exosomes are enriched in cholesterol; *e.g.* B lymphocytes release exosomes with a cholesterol-to-phospholipid ratio approximately three times higher compared with the parent cell membrane (9). This prompted us to investigate whether exosomes might contribute to the regulation of cellular cholesterol homeostasis by exosomal egress of cholesterol from the cell.

The tight regulation of cellular cholesterol is crucial for the structure, biophysical properties, and function of membranes. Cholesterol homeostasis is maintained by a balance between efflux, uptake, and endogenous synthesis of cholesterol (10). Sterols derive from mevalonate and are synthesized from isopentyl phosphate in the endoplasmic reticulum (ER) from where they are transported to the plasma membrane by a nonvesicular, energy-dependent mechanism. Exogenous cholesterol is either taken up via receptor-mediated endocytosis of LDL particles or by bulk flow endocytosis. LDL-derived sterol esters are hydrolyzed by acid lipase in acidic endosomal compartments, and free cholesterol is transported to late endosomes/lysosomes. From there, cholesterol egresses to various destinations, including the ER, trans-Golgi network, mitochondria, and plasma membrane (10, 11). The exit of free cholesterol from late endosomal/lysosomal compartments depends on two proteins, NPC1 and NPC2, that bind and transfer cholesterol (12, 13). Homozygous mutations in Niemann-Pick type C disease (NPC) result in accumulation of unesterified cholesterol and sphingolipids within the late endosomal and lysosomal compartments, preferentially of brain, liver, and spleen (14). Clinically, the storage disease is characterized by progressive

* This work was supported by grants from the Research Program, Faculty of Medicine, Georg-August-University Göttingen, Germany (Grant 0010/1401870 and Heidenreich-Siebold-Program (to A. S.)), the Center of Molecular Physiology of the Brain Göttingen and a Novartis fellowship (to A. S.), and by an European Research Council starting grant (to M. S.).

[S] The on-line version of this article (available at http://www.jbc.org) contains supplemental Figs. S1–S6.

[1] To whom correspondence should be addressed: Max-Planck-Institute for Experimental Medicine, Hermann-Rein-Str.3, 37075 Goettingen, Germany. Tel.: 49-551-396610; Fax: 49-551-396692; E-mail: aschnei8@gwdg.de.

[2] The abbreviations used are: MVB, multivesicular body; CRAC, cholesterol recognition/interaction amino acid motifs; ER, endoplasmic reticulum; mβ-CD, methyl-β-cyclodextrin; NPC, Niemann-Pick C; PLP, proteolipid protein; mβCD, methyl-β-cyclodextrin; EGFP, enhanced GFP; NPC disease, Niemann-Pick type C disease; flot-2, flotillin-2.

neurodegeneration and extensive dysmyelination of axons in the central nervous system (CNS) (15). However, the exact mechanism of how defects in NPC1 or NPC2 are detrimental to the cell is still unclear. A loss of function defect with diminished cholesterol transport to the plasma membrane and a gain of function effect with toxicity caused by late endosomal cholesterol accumulation have both been discussed (16). Here we show that exosomes can shuttle cholesterol out of the cell and partially bypass the late endosomal trapping of cholesterol observed in NPC disease.

EXPERIMENTAL PROCEDURES

Plasmids—The following plasmids were used: GFP-rab4, GFP-rab5, GFP-rab7 (M. Zerial, Max Planck Institute of Molecular Cell Biology and Genetics, Dresden, Germany), MLV Gag-GFP (Addgene plasmid 1813, W. Mothes, Yale University School of Medicine), pR4-PLP-myc, Flotillin-1-GFP, Flotillin-2-GFP, and Flotillin-2-RFP (L. Rajendran, Max Planck Institute of Molecular Cell Biology and Genetics, Dresden, Germany), EGFP-CD63 (D. Cutler, University College, London, UK), and pEYFP-His_6-wtNPC1, pEYFP-His_6-NPC1 P692S (M. Scott, Stanford University, Stanford, CA). Flotillin-2 CRAC mutants were generated by site-directed mutagenesis to introduce Y124G, Y163G, and the Y124G/Y163G double mutant according to the manufacturer's protocol (QuikChange site-directed mutagenesis kit, Stratagene, CA).

Antibodies—Primary antibodies were: anti-Myc (monoclonal IgG, Cell Signaling), mouse monoclonal antibodies against flotillin-1 and flotillin-2, monoclonal rat anti-LAMP-1 (BD Biosciences), rabbit anti-NPC1 (Novus Biologicals, Littleton, CO), rabbit anti-GFP (Abcam), mouse anti-tsg 101 (anti-tumor susceptibility gene 101) (Abcam), mouse anti-alix (BD Biosciences). Secondary antibodies were obtained from Dianova, Invitrogen, and GE Healthcare.

Immunofluorescence and Filipin Staining—Immunofluorescence labeling was performed according to a standard protocol. For filipin labeling, cells were fixed with 4% paraformaldehyde before staining with filipin (Sigma) in phosphate-buffered saline.

Cell Culture, Transfection, and siRNA Delivery—The oligodendroglial precursor cell line Oli-neu was provided by J. Trotter, University of Mainz, Germany, and cultured as described (17). Primary human skin fibroblasts were cultured from skin biopsies of a healthy volunteer and a patient with clinical symptoms suggesting NPC disease (NPC-db patient ID #158) (18). Filipin stainings of cultured cells were performed as described and showed a "variant" filipin phenotype in the patient, suggesting moderate cholesterol enrichment (15). Molecular genetic analysis of the full coding region of *npc1* revealed compound heterozygosity for *npc1* mutations p.P1007A (c.3019C>G) in exon 20 and p.R934*X* (c.2800C>T) in exon 19 of the *npc1* gene. Analysis with patient material was approved by the ethical committee of the Medical Faculty, University of Heidelberg. Both subjects enrolled gave their written informed consent. Fibroblast cultures were cultivated in DMEM, 10% FCS. Wild-type and CT43 Chinese hamster ovary (CHO) cells were kindly provided by T. Y. Chang (Dartmouth Medical School, Hanover, NH) and cultivated in DMEM, 10% FCS. The CT43 line contains a truncation mutation in the NPC1 protein after amino acid 933, which results in a complete loss of NPC1 function (19). Transient transfections of Oli-neu or CHO cells were performed with FuGENE transfection reagent (Roche Applied Science) or TransIT transfection reagent (Mirus Bio LLC, Madison, WI) according to the manufacturer's protocol.

RNA oligonucleotides were delivered into Oli-neu cells by electroporation with a basic neuron kit following the manufacturer's instructions (Lonza, Cologne, Germany). Nucleofection was repeated after 48 h, and experiments were performed after an additional 48 h period. The following siRNAs were used: mouse flotillin-2, GUUCAUGGCAGACACCAAdTdT (Qiagen); mouse NPC1:_Mn_NPC1–1 predesigned siRNA (Qiagen). Control siRNA was obtained from Ambion (Austin) (Control siRNA #1).

Cholesterol Depletion/Loading—All experiments were carried out in lipoprotein-free serum (LPS)-supplemented medium (Sigma). For acute cholesterol depletion, cells were washed 3 times with Hanks' balanced salt solution followed by a 2-h incubation with 1 mM methyl-β-cyclodextrin (mβCD) in Hanks' balanced salt solution at 37 °C. For inhibition of HMG-CoA reductase, we preincubated cells with medium supplemented with LPS for 24 h. Cells were subsequently treated with 4 μM simvastatin plus 50 μM L-mevalonate to maintain geranylation and farnesylation over a time period of 16 h.

Free cholesterol was added to the cells at a final concentration of 50 μg/ml as mβCD complex (Sigma) saturated with 10 μg/ml cholesterol dissolved in ethanol (final concentration of ethanol 0.1%). Acyl-coenzyme A:cholesterol acyltransferase inhibitor CP-113.818 was kindly provided by Pfizer and added to the cells at a final concentration of 10 μM. U18666A was purchased from Biomol (Plymouth Meeting) to treat cells at a final concentration of 1.5 μg/ml for 16 h in normal growth medium.

Microscopy and Analysis—Fluorescence images were acquired on a Leica DMRXA microscope or a Zeiss LSM 510 confocal microscope with a 63× oil plan-apochromat objective (NA 1.4; Carl Zeiss, Jena, Germany). Image processing and analysis were performed using Meta Imaging Series 6.1 software (Universal Imaging Corp.). Fluorescence intensities were quantified as reported previously by Metamorph Imaging software (20). For electron microscopy analysis, exosomes were prepared from Oli-neu cells. and the 100,000 × *g* fraction was fixed with 4% paraformaldehyde. The fraction was adsorbed to glow-discharged Formvar-carbon-coated copper grids by floating the grid for 10 min on 5-μl droplets on Parafilm. The grids were negatively stained with 2% uranyl acetate containing 0.7 M oxalate, pH 7.0, and imaged with a LEO EM912 Omega electron microscope (Zeiss, Oberkochen). Digital micrographs were obtained with an on-axis 2048 × 2048 CCD camera (Proscan, Scheuring).

Endocytosis Assays and Quantification—To quantify flotillin distribution, cells were fixed with paraformaldehyde and immunostained for flotillin. Confocal images were taken with identical acquisition parameters, and fluorescence intensities of cell-membrane *versus* intracellular vesicular flotillin were measured by Metamorph software as described previously (21).

The ratio of cytosolic/total fluorescence intensity was calculated for each cell.

Exosome Purification and Western Blotting—Exosomes were prepared as described previously (22). Briefly, cells were grown on plastic dishes. The medium was removed, and cells were washed three times with Hanks' balanced salt solution before the addition of serum-free medium for a time period of 4–16 h. Culture media was collected and centrifuged for 10 min at 3,000 × *g* followed by centrifugation twice at 4,000 × *g* and one 30-min 10,000 × *g* centrifugation step before a 1-h ultracentrifugation at 100,000 × *g*. The pellet was resuspended in sample buffer and subjected to SDS-PAGE electrophoresis, transferred to nitrocellulose membranes that were incubated with the respective primary and secondary antibodies, and developed with enhanced chemiluminescence kit (ECL, Amersham Biosciences). The corresponding parent cells were scraped into lysis buffer (1% CHAPS, 5 mM EDTA, 50 mM Tris, pH 8.0), and the postnuclear supernatants were dissolved into sample buffer and analyzed by Western blotting. The blots were scanned and quantified by ImageJ to calculate the ratio of protein in the exosomal *versus* the total cellular fraction.

Sucrose Gradient Ultracentrifugation—Exosomes were purified from culture medium through a sequence of centrifugation steps as described above. For sucrose gradient ultracentrifugation, the 100,000 × *g* pellet was resuspended in 400 μl of 0.25 M sucrose in 10 mM HEPES, pH 7.4, and layered on top of a discontinuous sucrose density gradient (total of 8 fractions, each 400 μl, 0.25–2.5 M sucrose, 10 mM HEPES, pH 7.4). After 18 h of centrifugation at 200,000 × *g* (SW60 rotor; Beckman Instruments), each fraction was diluted 1:6 with PBS, and recentrifuged at 100,000 × *g* for 1 h. The pelleted material from each fraction was resuspended in sample buffer and analyzed by Western blotting.

Cholesterol Determination—Exosome fractions and the corresponding cell lysates were resuspended in equal amounts of cold Tris-EDTA buffer, and cholesterol was extracted. Briefly, lanosterol was added as an internal standard for quantification, and samples were kept at 4 °C for 30 min with methanol/chloroform under constant shaking. After the addition of chloroform and H_2O, the mixture was left on ice for another 15 min before centrifugation for 15 min at 4 °C and 13,000 × *g*. The lower organic phase was transferred to a glass tube, dried under streaming nitrogen, and subjected to gas chromatography. The analysis was performed with an Agilent (Waldbronn, Germany) 6890 gas chromatograph fitted with a capillary HP-5 column (30 m × 0.32 mm; 0.25-μm coating thickness; J&W Scientific, Agilent). Helium was used as carrier gas (1 ml/min). The temperature gradient was 200 °C for 1 min, 200–325 °C at 20 °C/min, and 325 °C for 7.5 min. Identity of cholesterol signal was verified with an authentic standard.

RESULTS

Cholesterol Regulates the Cellular Distribution of Flotillin—Flotillin is a cytosolic, membrane-associated protein involved in scaffolding functions, signaling, and endocytosis (23, 24). Its two isoforms, flotillin-1 and flotillin-2, are enriched in exosomes and can be used as protein markers to quantify exosomal release (22). Flotillin can recruit cholesterol to the plasma membrane and intracellular membranes, where it colocalizes with cholesterol (25, 26). Therefore, we examined whether trafficking and exosomal secretion of flotillin is regulated by cholesterol.

Subcellular Localization of Flotillin—In the mouse oligodendroglial cell line Oli-neu, immunofluorescence labeling with an antibody directed against flotillin-2 revealed a predominantly vesicular staining pattern on confocal sections. Only a minor fraction of flotillin-2 was detected at the plasma membrane. Expression of different GFP-tagged rab-GTPases and immunostaining of endogenous flotillin-2 showed colocalization of flotillin-2 with markers of early endosomes (GFP-rab5), recycling endosomes (GFP-rab4), and the late endosome/lysosome system (GFP-rab7, LAMP-1, and lysotracker colocalization) (data not shown).

Cholesterol Depletion Redistributes Flotillin to the Plasma Membrane—Recently, a flotillin-dependent endocytosis pathway regulated by cholesterol has been identified (27). In accordance with these results we found that the distribution of flotillin between the plasma membrane and intracellular compartments was cholesterol-dependent. Acute depletion of plasma membrane cholesterol by 2 h of treatment with 1 mM mβCD resulted in a modest accumulation of flotillin-2 at the plasma membrane as shown by confocal microscopy images (8.6% shift from endosomal pools to the plasma membrane, S.E. = 0.02, $n = 220$ cells, $p = 0.002$, Student's t test, 2 independent experiments) (supplemental Fig. S1, *A* and *D*). A similar distribution was obtained for flotillin-1 (data not shown). Statins inhibit HMG-CoA reductase, the key enzyme in cholesterol biosynthesis, which catalyzes the production of L-mevalonate. However, reduction of L-mevalonate also impairs the geranylation and farnesylation of various proteins, which play a crucial role in various cellular functions. To exclude any cholesterol-independent effects, we treated cells with a combination of 4 μM simvastatin and 50 μM L-mevalonate in LPS-supplemented medium for 48 h before fixation (28). Similar to our results observed after acute cholesterol depletion, we detected a redistribution of flotillin-2 and flotillin-1 from the endosomal pool to the plasma membrane (23.4% decrease of flotillin-2, S.E. = 0.013, $n = 175$ cells, $p < 0.0001$, Student's t test, 2 independent experiments) (supplemental Fig. S1, *B* and *D* and data not shown).

Accumulation of Flotillin in the Endosomal Pool after Loading of Free Cholesterol—The addition of free cholesterol to the medium of cells that were starved for 4 h in LPS resulted in a shift of flotillin-2 from the plasma membrane to endosomal pools (13.6% increase, S.E. = 0.028, $n = 171$ cells, $p = 0.0003$, Student's t test, 2 independent experiments) (supplemental Fig. S1, *C* and *D*).

After treatment with cholesterol, we observed a pronounced vesicular filipin staining of cells in contrast to the homogenous staining of control cells, indicating that the cholesterol loading protocol leads to intracellular cholesterol accumulation in cytoplasmic vesicles (supplemental Fig. S2*A*). Filipin-positive compartments partially colocalized with endogenous flotillin-2, the late endosomal marker protein GFP-rab7, the lysosomal marker LAMP, and EGFP-CD63, suggesting that cholesterol might traffic on the same endocytic itinerary as flotillin-2 (supplemental Fig. S2, *B*–*E*).

U18666A inhibits the transport of cholesterol from lysosomes to other cellular sites, resulting in lysosomal accumulation of cholesterol. After U18666A treatment we found an accumulation of flotillin-2 within vesicular compartments, where it might have been trapped together with cholesterol (7.06% increase, S.E. = 0.02, $n = 69$ cells, $p = 0.022$, Student's t test, 2 independent experiments) (supplemental Fig. S2*F*). Similar findings were obtained after inhibition of acyl-coenzyme A:cholesterol acyltransferase, the enzyme catalyzing the esterification of free cholesterol to fatty acids in the ER. After a 24-h incubation of Oli-neu cells with the acyl-coenzyme A:cholesterol acyltransferase inhibitor CP-113.818, we found an increased ratio of intracellular to plasma membrane flotillin-2 and flotillin-1 (21.8% increase, S.E. = 0.025, $n = 213$ cells, $p < 0.0001$, Student's t test, 2 independent experiments) (supplemental Fig. S2*G* and data not shown). We, therefore, reasoned that free cholesterol transport within the cell might be closely related to flotillin trafficking.

Flotillin Interacts with Cholesterol by Two Cholesterol Recognition/Interaction Domains—Two putative cholesterol recognition/interaction amino acid motifs (CRAC; (L/V-(X)(1-5)-Y-(X)(1-5)-R/K)) have been predicted for flotillin-2 which might enable it to bind and sequester cholesterol at the membrane (26). The functionality of CRAC domains has been previously demonstrated in the translocator protein, also known as peripheral type benzodiazepine receptor, a protein that plays a role in cholesterol import into mitochondria (29, 30). The mutation of a tyrosine residue in the translocator protein CRAC domain was described to exert a negative impact on cholesterol uptake and translocation into mitochondria (30). To test the functionality of CRAC domains in flotillin-2, we introduced point mutations into one or both putative CRAC motifs spanning amino acids 120–127 (VEQIYQDR) and amino acids 157–169 (VYDKV-DYLSSLGK) of flotillin-2-GFP (flotillin-2-GFP Y124G, flotillin-2-GFP Y163G, and flotillin-2-GFP Y124G/Y163G). Fig. 1 demonstrates the marked accumulation of all CRAC mutants at the plasma membrane of transfected cells, which was the most prominent in the case of flotillin-2-GFP Y124G and the double mutant flotillin-2-GFP Y124G/Y163G (51% reduction, S.E. = 0.05, $p < 0.0001$, Student's t test, 3 independent experiments). Our findings indicate that translocation of flotillin-2 from the plasma membrane to endocytic compartments depends on at least one of this protein CRAC domains.

Flotillin-2-positive Exosomes Are Released in a Cholesterol-dependent Fashion—Flotillin is enriched in exosomes; however, the exact mechanisms regulating exosomal biogenesis and release are not fully understood. Given the cholesterol dependence of flotillin endocytosis and trafficking within the endosomal system, we wondered whether cholesterol might also influence the exosomal release of flotillin. We, therefore, starved Oli-neu cells for 4 h in medium supplemented with lipoprotein-free serum before exchange of medium and the addition of a water-soluble cholesterol-mβCD complex saturated with ethanol-dissolved free cholesterol in serum-free medium. Control cells were treated with ethanol only. No visible cytotoxicity was observed. After 4 h, the medium was collected, and the exosomal fraction was purified by subsequent centrifugation steps to clear the medium from cells and cellular debris before purification of exosomes by centrifugation at 100,000 × *g* as described before in Oli-neu cells (22). Pellets from each subsequent centrifugation step were subjected to Western blotting and detected with an antibody against flotillin-2 to show enrichment of flotillin-2 in the 100,000 × *g* pellet (supplemental Fig. S3*A*). For further purification and analysis of the 100,000 × *g* fraction, we subjected the pellet to sucrose gradient ultracentrifugation. Pelleted material from each fraction was analyzed by Western blotting. Flotillin-2 immunoreactivity was exclusively recovered from 1.11–1.16 g/ml density fractions, similar to the exosomal marker proteins tsg 101 (tumor susceptibility gene 101) and alix (supplemental Fig. S3*A*). Size and density of the 100,000 × *g* pellet material are similar to that described for other exosomal preparations (7). The electron micrographs obtained from the 100,000 × *g* pellet preparation further verify the typical vesicular structures of exosomes with a 50–90-nm diameter (supplemental Fig. S3*B*). Although we found a robust signal for the exosomal marker proteins flotillin-2 and alix in the 100,000 × *g* pellet (supplemental Fig. S3*C*), no immunoreactivity was detected with the ER marker protein calnexin or the trans-Golgi network resident protein γ-adaptin, indicating the absence of microsomal contamination of the 100,000 × *g* pellet (supplemental Fig. S3*C*). In the following text we refer to this 100,000 × *g* pellet fraction as the exosomal fraction.

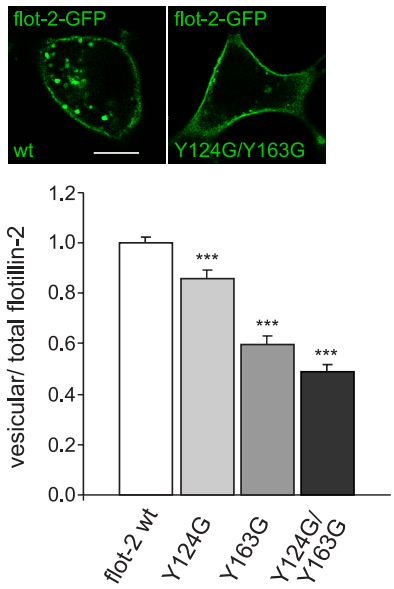

FIGURE 1. **The CRAC domains of flotillin-2 (*flot-2*) are required for intracellular vesicular localization of the protein.** Flot-2-GFP wild type or flot-2-GFP bearing point mutations in one or two putative CRAC domains (Y124G, Y163G, and Y124G/Y163G) were transfected into Oli-neu cells (immunofluorescence, *upper panel*). The quantification of vesicular to total cellular flotillin-2-GFP (wild-type or mutants Y124G, Y163G, Y124G/Y163G) (histogram, *lower panel*) reflects the accumulation of CRAC mutants at the plasma membrane. Note that the double mutation of both CRAC domains Y124G/Y163G in flotillin-2-GFP (*right*) exerts the most pronounced effect compared with wild-type flot-2-GFP (*left*). Values are given as means ± S.E. from three independent experiments. *** indicates $p < 0.0005$. *Scale bar*, 10 μm.

Exosome release was measured by calculating the ratio of 100,000 × *g* pelleted material, *i.e.* the exosomal fraction, to cellular flotillin-2 levels, determined by image analysis of the respective scanned blots. As shown in Fig. 2*A*, exosomal release

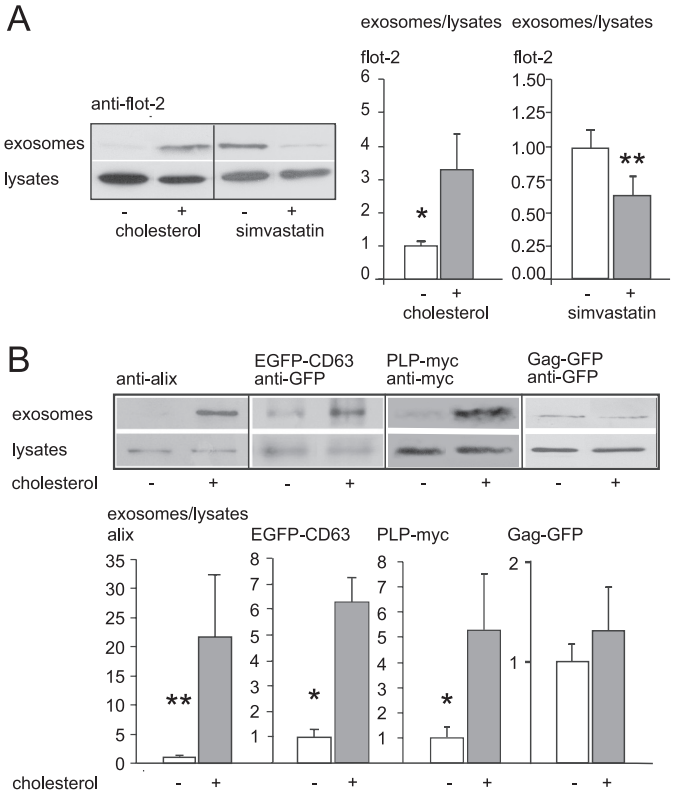

FIGURE 2. **Cholesterol enhances the release of flotillin-2-positive exosomes.** *A*, Western blot and quantification of exosomal release after cholesterol loading of Oli-neu cells (*left part of the blot*, *gray bar*) or mock-treated control cells (*white bar*) are shown. Blots were scanned, and the ratio of endogenous flotillin-2 intensity in the exosomal fraction to flotillin-2 intensity in the cell lysates of exosome secreting parent cells was determined. Similarly, exosome release was determined after treatment of Oli-neu cells with simvastatin (*right part of the blot*, *gray bar*) compared with untreated controls (*white bar*). Values are given as the mean ± S.E. from $n = 8$ and $n = 12$ experiments. *B*, shown are Western blots (*top panel*) and quantification (*bottom panel*) of exosomal release of endogenous alix, transiently expressed EGFP-CD63, PLP-myc, and Gag-GFP after cholesterol loading (*gray bars*) or not (*white bars*, normalized to 1) in Oli-neu cells. Values are given as the mean ± S.E. from $n = 6, 4, 5$, and *12* experiments. Similar to flotillin-2, alix, EGFP-CD63, and PLP-myc immunoreactivity was increased in the 100,000 × *g* fraction after cholesterol treatment, whereas cholesterol has no significant impact on the release of Gag-GFP within exosome-like particles. *, $p < 0.05$; **, $p < 0.005$.

determined by the marker flotillin-2 significantly increased upon cholesterol loading (increase to 320%, S.E. = 110%, $n = 8$, $p = 0.022$, Mann-Whitney *U* test). In contrast, 24 h of lipoprotein depletion followed by another 16 h of simvastatin treatment (4 μM plus 50 μM L-mevalonate) to decrease cellular cholesterol resulted in a significant reduction of exosome-associated flotillin-2 release (37.54% decrease, S.E. = 14%, $n = 17$, $p = 0.0019$, Mann-Whitney *U* test) (Fig. 2*A*). To rule out that cholesterol treatment induced shedding of flotillin-2-positive apoptotic vesicles that would co-sediment with exosomes, we performed sucrose gradient analysis of the 100,000 × *g* pellet. As shown in supplemental Fig. S3*D*, flotillin-2 immunoreactivity was recovered from identical fractions (1.11 and 1.16 g/ml) under both conditions.

The increase of flotillin-2 intensity in the 100,000 × *g* fractions could either be due to a modification of the trafficking of flotillin-2 to exosomes or due to up-regulation of exosomal release *per se*. To distinguish between these two possibilities, we determined the cholesterol-induced enrichment of two other exosomal marker proteins, alix and CD63, in the 100,000 × *g* pellet. Similar to flotillin-2, both endogenous alix and transiently transfected EGFP-CD63 were significantly enriched in the 100,000 × *g* fraction after treatment with cholesterol (alix: increase to 2149.29%, S.E. = 1066.12%, $n = 6$, $p = 0.004$, Mann-Whitney *U* test; EGFP-CD63: 628.30% increase, S.E. = 93.77%, $n = 4$, $p = 0.021$, Mann-Whitney *U* test) (Fig. 2*B*). The enrichment of several exosomal proteins in response to cholesterol treatment indicates that cholesterol increases exosomal release rather than the number of flotillin molecules per exosomal vesicle. To strengthen our results on cholesterol-induced exosomal secretion, we examined the secretion of two other exosomal marker proteins in response to cholesterol. The proteolipid protein (PLP) is a transmembrane protein that, similar to flotillin, is localized at the plasma membrane and in the endosomal system (26). When we transfected PLP-myc in Oli-neu cells, we detected a marked colocalization with flotillin-2 at the plasma membrane and in the endosomal compartment (supplemental Fig. S4*A*). The Moloney murine leukemia virus Gag protein is a matrix protein that resides at the plasma membrane where it can be released in virus-like particles by direct shedding from the plasma membrane, a pathway that has been described as the immediate way of exosome budding (31). Exogenously expressed Gag-GFP colocalizes rarely with endogenous flotillin-2 in Oli-neu cells (supplemental Fig. S4*B*).

We assessed the effect of cholesterol loading on the exosomal release of the two proteins PLP-myc and Gag-GFP. Exosomal PLP-myc secretion responded in a similar way to cholesterol as flotillin-2, alix, and EGFP-CD63, whereas Gag-GFP was not significantly affected by cholesterol levels (PLP-myc: increase to 526.8%, S.E. = 223%, $n = 5$, $p = 0.03$, Mann-Whitney *U* test; Gag-GFP: 36.4% increase, S.E. = 0.45%, $n = 12$, $p = 0.27$, Mann-Whitney *U* test) (Fig. 2*B*). These results point toward a cholesterol dependence of the delayed exosome pathway, in contrast to the immediate pathway, the latter not being affected by cholesterol.

This is further supported by our finding that the cholesterol-triggered exosomal release of CRAC double-mutant flotillin-2-GFP Y124G/Y163G, which lacks the cholesterol recognition domains and localizes predominantly to the plasma membrane, is significantly lower than that of wild-type flotillin-2 (54.48% decrease, S.E. = 7.6%, $n = 13$, $p = 0.0136$, Student's *t* test) (Fig. 3).

Flotillin Regulates Exosomal Cholesterol Release—Having shown that flotillin trafficking and exosomal release depend on cholesterol levels, we wondered whether flotillin might play a role in cellular cholesterol homeostasis. To address this question, we down-regulated its expression by a flotillin-2-specific siRNA. Flotillin-2 forms hetero-oligomers with flotillin-1, a process that is required for the stability of the flotillin-1 isoform. As previously shown, the siRNA-mediated knockdown of flotillin-2 results in degradative down-regulation of flotillin-1 (32). Flotillin-2 siRNA and control siRNA-transfected cells were incubated with cholesterol in serum-free medium after a 4-h period of starving (for quantification of knockdown efficiency, see Fig. 4*B*). Medium was collected for purification of exosomes from treated and untreated cells. Exosomes and the corresponding parent cells were dissolved in Tris-EDTA buffer

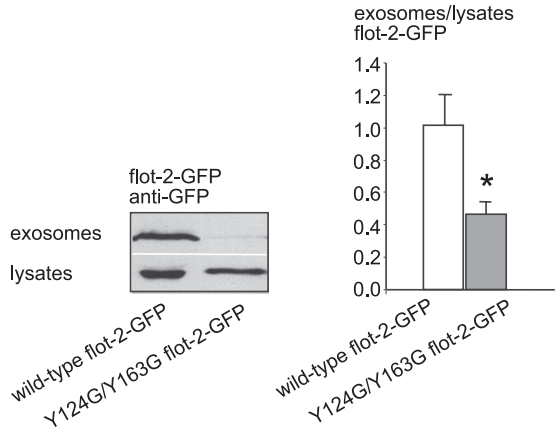

FIGURE 3. **The CRAC domains of flotillin-2 are necessary for exosomal release of the protein.** Shown are Western blot of lysates (*lower panel*) and exosome fractions (*upper panel*) from Oli-neu cells transfected with flotillin-2-GFP wild-type (*left*) and CRAC double mutant flotillin-2-GFP Y124G/Y163G (*right*). Blots were scanned, and the intensity of bands was quantified. The histogram shows the ratio of exosomal wild-type flotillin-2-GFP (*white bar*) and CRAC double mutant flotillin-2-GFP intensities (*gray bar*) to respective cell lysates after cholesterol loading of the cells. Controls were normalized to 1. Values are given as the mean ± S.E. from $n = 13$ experiments. * indicates $p < 0.05$.

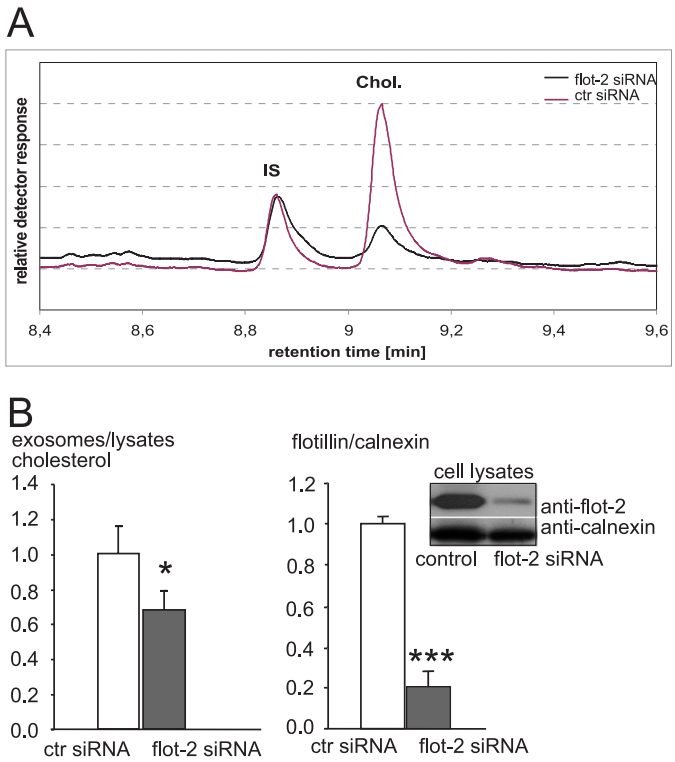

FIGURE 4. **Flotillin is required for exosomal release of cholesterol.** Oli-neu cells were transfected with siRNA directed against flotillin-2 or with control siRNA. *A*, the organic phase was extracted from exosomal fractions and parent cell lysates and subjected to gas chromatography to quantify cholesterol contents. A typical retention profile is shown for exosome fractions from flotillin-2 knockdown cells (*black*) and control cells (*lilac*). *IS*, internal standard. *B*, the *left histogram* depicts the cholesterol ratio from exosomes *versus* parent cell lysates after siRNA-mediated down-regulation of flotillin-2 (*gray bar*) or from control (*ctr*) siRNA-transfected cells (*white bar*). Values of controls were normalized to 1, and all values are given as the mean ± S.E. from $n = 5$ experiments. * indicates $p < 0.05$. The *right histogram* and *Western blot* show siRNA-mediated down-regulation of flotillin-2. Cells were scraped into lysis buffer and subjected to Western blotting. Down-regulation of flotillin-2 was determined by probing the blot membrane with antibodies against flotillin-2 (*upper lane*) and calnexin (*lower lane*) as an internal standard. The ratio flotillin-2 to calnexin is shown for treatment with control siRNA (*white bar*) and flotillin-2 siRNA (*gray bar*). Values are given as the means ± S.E. for $n = 9$ experiments. *** indicates $p < 0.0005$. The knockdown efficiency was ~80%.

before cholesterol was extracted and measured by gas chromatography (Fig. 4*A*). The ratio of exosomal to cellular cholesterol was significantly reduced in flotillin-2 siRNA-treated cells (33.38% reduction, S.E. = 13.21, $n = 8$, $p = 0.03$, Mann-Whitney *U* test) (Fig. 4*B*). This suggests a role for flotillin in the release of cholesterol in association with exosomes.

Exosomal Cholesterol Release Is Up-regulated in NPC—Because cholesterol loading enhanced exosome release, we examined whether exosomal secretion of cholesterol might be up-regulated in NPC disease, which is characterized by intracellular accumulation of free cholesterol. To this aim, we treated Oli-neu cells with U18666A, which traps cholesterol in the late endosomal/lysosomal compartments and mimics the trafficking defect observed in NPC (33). When we compared exosome release between U18666A-treated and control cells, we found a dramatic increase of exosome secretion after 16 h of U18666A treatment as determined by flotillin-2, alix, and transiently transfected EGFP-CD63 (flotillin-2: increase to 307%, S.E. = 77%, $n = 8$, $p = 0.02$, Student's *t* test; alix: increase to 262%, S.E. = 105.1%, $n = 15$, $p = 0.046$, Mann-Whitney *U* test; EGFP-CD63: increase to 188%, S.E. = 60%, $n = 15$, $p = 0.095$, Mann-Whitney *U* test) (Fig. 5*A*). We next determined the amount of cholesterol released after incubating cells with U18666A. As shown in Fig. 5*B*, cholesterol secretion within exosomes is significantly up-regulated by preventing cholesterol egress from the late endosomal/lysosomal compartments with U18666A (78% increase, S.E. = 13.4%, $n = 9$, $p = 0.0049$, Mann-Whitney *U* test). In contrast, the accumulation of free cholesterol in the ER obtained by inhibition of cholesterol esterification with an inhibitor of the enzyme acyl-coenzyme A:cholesterol acyltransferase (CP-113.818) had no impact on exosome secretion (4.20% decrease, S.E. = 6.11%, $n = 5$, $p = 0.5$, Mann-Whitney *U* test) (Fig. 5*C*). This hints to a specific bypass mechanism that prevents toxic cholesterol accumulation in the late endosomal system. However, it cannot be excluded that CP-113818, which in addition to inhibiting acyl-coenzyme A:cholesterol acyltransferase activity, also intercalates into membrane lipid bilayers, could interfere with budding of intraluminal vesicles by changing the membrane properties, thereby interfering with exosome biogenesis and release (34).

Our findings prompted us to investigate whether exosomes might fulfill a function in NPC disease. NPC1 is a 170–190-kDa glycoprotein comprising 13 transmembrane domains and a sterol-sensing domain between transmembrane domains 3 and 7. It has recently been shown that NPC2 shuttles free cholesterol either to or from NPC1. In the first case, the intraluminal protein NPC2 would bind free cholesterol derived from acid lipase and transfer it to membrane-bound NPC1 within the lysosomal membrane (35–38). From there, NPC1 would directly shuttle cholesterol to the ER. Alternatively, NPC1 could bind cholesterol after release from acid lipase and transfer it to NPC2, which might mediate the insertion of cholesterol into the lyso-

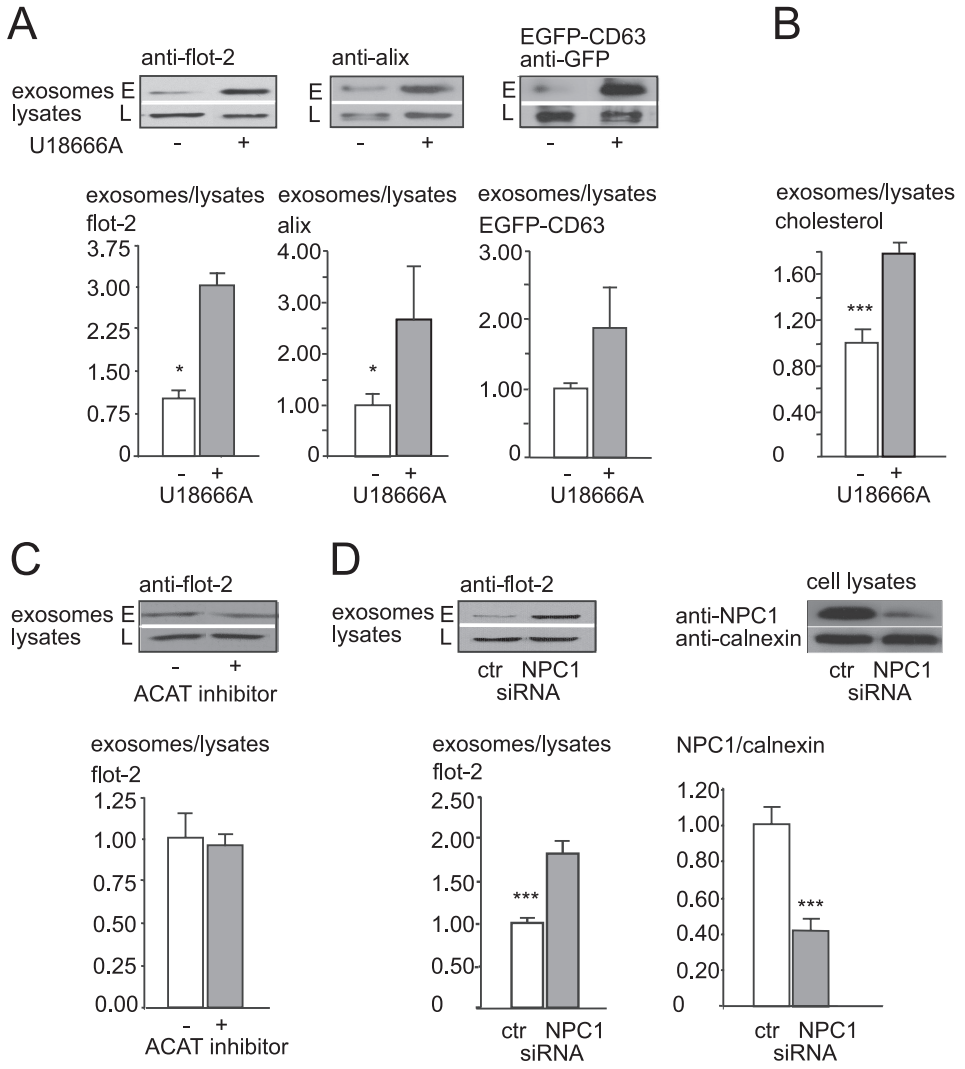

FIGURE 5. **Exosome release is up-regulated by pharmacological trapping of cholesterol in the late endosome or down-regulation of Niemann-Pick type C protein.** *A*, shown is exosome release from Oli-neu cells treated with U18666A (*gray bar*) or not (*white bar*), determined as the ratio of endogenous flotillin-2 (*left*), alix (*middle*), and transiently transfected EGFP-CD63 (*right*) in the exosome fraction (*E*) *versus* corresponding cell lysates (*L*). *B*, a similar experiment as in *A* is shown. Cells were treated with U18666A or solvent only. Cholesterol contents of exosome fractions and cell lysates were determined by gas chromatography. The ratio of cholesterol in exosomes to parent cell lysates is shown for U18666A treated cells (*gray bar*) and controls (*white bar*). *C*, exosome release from Oli-neu cells untreated (*white bar*) or treated (*gray bar*) with acyl-coenzyme A:cholesterol acyltransferase (*ACAT*) inhibitor CP-113.818 is shown as a ratio of flotillin-2 in the exosomal fraction to corresponding cell lysates. *D*, exosome release from Oli-neu cells either treated with siRNA directed against NPC1 (*gray bar*) or control (*ctl*) siRNA (*white bar*) is shown. Flotillin-2 was used as marker protein for quantification of exosome release as ratio of flotillin-2 in the exosome fraction to corresponding cell lysates. The *right histogram* and *Western blot* shows siRNA-mediated down-regulation of NPC1. Cells were electroporated with control siRNA (*left lane*) or NPC1 directed-siRNA (*right lane*), and lysates were probed with an antibody recognizing endogenous NPC1 (*upper panel* of the Western blot). The same blot membrane was incubated with an antibody directed against calnexin (*lower panel*). Knockdown efficiency of NPC1-directed siRNA was calculated as the ratio of NPC1 to calnexin intensity of control siRNA (*white bar*)- or NPC1 siRNA (*gray bar*)-treated cells. Values are given as the means ± S.E. from $n = 8$ experiments with controls normalized to 1. *** indicates $p < 0.0005$.

somal membrane. An as yet unknown cholesterol transporter could then release cholesterol to the ER (39).

When we down-regulated NPC1 by siRNA in Oli-neu cells (Fig. 5*D*) and measured exosome release, we found a significant increase in exosome secretion compared with control siRNA (82.1% increase, S.E. = 16.5%, $n = 9$, $p = 0.001$, Mann-Whitney *U* test) (Fig. 5*D*). More than 200 disease-causing mutations have been identified so far in the *npc1* gene. We incubated primary human fibroblasts from patients harboring the compound heterozygous R934*X*/P1007A mutation as well as fibroblasts from healthy controls under lipoprotein-depleted serum conditions for 24 h before full medium was added to achieve high vesicular cholesterol accumulation as shown by filipin staining and quantification in Fig. 6*A*. After 24 h, cells were washed 3 times in Hanks' balanced salt solution and incubated in serum-free medium. Medium was collected over 4 h, and exosome release was quantified as flotillin-2 ratio of exosome preparations to cell lysates. As depicted in Fig. 6*B*, fibroblasts from patients bearing the NPC1 mutation R934*X*/P1007A released a significantly higher amount of exosomes than fibroblasts from healthy control fibroblasts (increase to 477.15%, S.E. = 236.56%, $n = 10$, $p = 0.0044$, Mann-Whitney *U* test). The same Western blots were additionally probed with an antibody against calnexin, and the ratio flotillin-2 to calnexin was calculated to rule out differences in cellular flotillin concentrations. Cellular flotillin-2 concentrations were not altered in NPC1 mutants compared with wild-type fibroblasts (data not shown). The exosome preparation from fibroblast medium was additionally incubated with antibodies against another exosomal marker protein, tsg101, and calnexin as a negative control (supplemental Fig. S5 and data not shown).

To test whether the effect of mutant NPC1 could be reverted by wild-type NPC1, we took advantage of the CHO cell line CT43, which contains a truncation mutation of the protein NPC1 after amino acid 933 (19). CT43 cells are derived from 25RA cells, which carry a gain of function mutation in the protein SCEBP cleavage-activating protein (SCAP) (40). However, during propagation of the originally described CT43 clone, the mutant SCAP allele reverted to a normal allele.[3] Therefore, we chose CHO wild-type cells instead of 25RA CHO cells as a control. A characterization of the 100,000 × *g* exosomal fraction and respective sucrose gradients is illustrated in

[3] T. Y. Chang, personal communication.

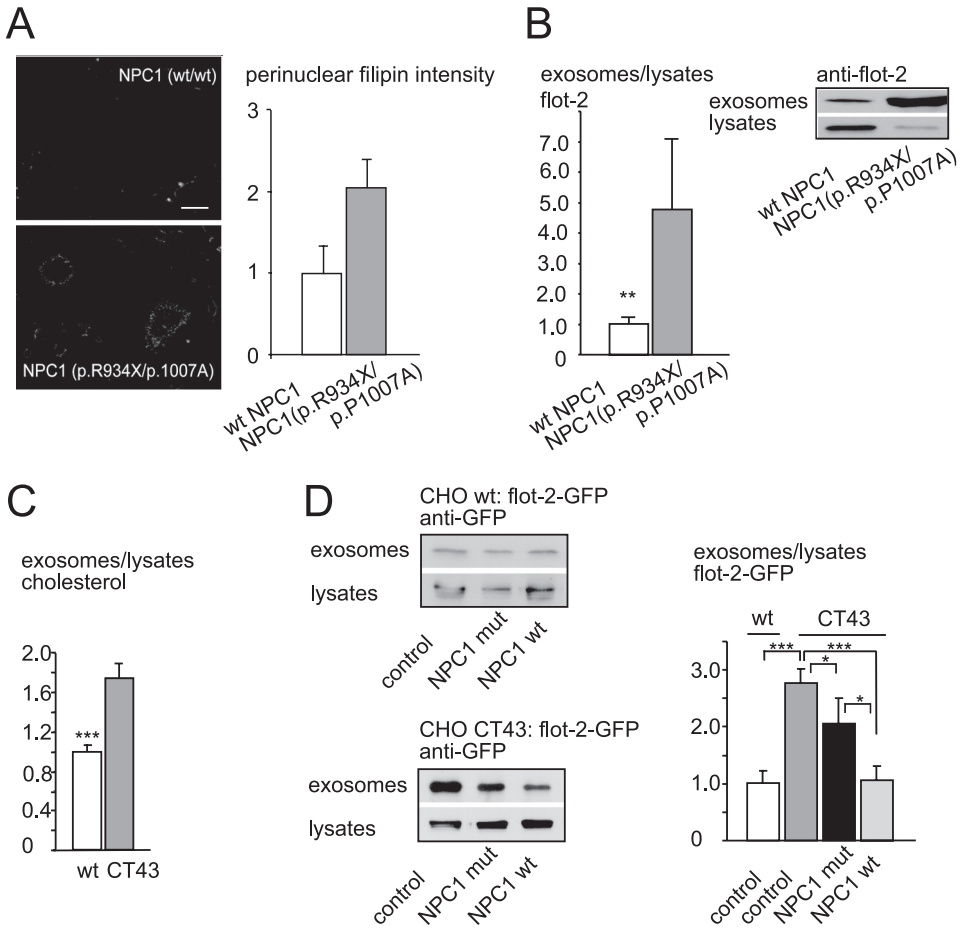

FIGURE 6. **Exosome secretion and exosomal cholesterol release are increased in Niemann-Pick type C disease.** *A*, filipin staining of human skin fibroblast cultures of a patient positive for the R934*X*/P1007A mutation (*bottom*) and wild-type control (*top*) is shown. Images were acquired automatically on a wide-field microscope using 10× objective. *Scale bar*, 10 μm. *Histogram*: perinuclear filipin signal intensities (arbitrary units) from up 200 individual cells/cell line were acquired and quantified as described by Bartz *et al.* (18) with modifications for cultured fibroblasts (H. Runz, unpublished results). *B*, exosome secretion by fibroblasts from NPC1 patients positive for the R934*X*/P1007A mutation (*gray bar*) and healthy controls (*white bar*) is shown. *Western blots*, the *upper two panels* show exosome fractions and cell lysates of fibroblasts from a patient positive for the R934*X*/P1007A mutation (*right*) and a healthy control (*left*) probed with an antibody against flotillin-2. All values are given as the mean ± S.E. from at least nine experiments. *C*, *histogram*, the ratio of cholesterol from exosomes *versus* parent cell lysates is increased in the CHO CT43 cell line (*right*), which carries a truncation mutation in the NPC1 protein compared with wild-type control CHO cells (*left*). *D*, Western blot of exosomes and lysates prepared from either wild-type CHO cells (*upper panel*) or the CHO CT43 cell line (*lower panel*). Cell lines were transiently transfected with flotillin-2-GFP alone (*left*) or in combination with mutant NPC1 P692S (*middle*) or wild-type NPC1(*right*). Blots were probed with anti-GFP antibody, and the ratio of flotillin-2-GFP in the 100,000 × *g* pellet *versus* lysates was quantified (*histograph*, *right*). *, $p < 0.05$; **, $p < 0.005$; ***, $p < 0.0005$. *mut*, mutant.

supplemental Fig. S6*A*. As shown in Fig. 6*C*, we found a significant increase of flotillin-2-GFP-positive exosomes as well as of exosomal cholesterol in medium collected for 5 h from the NPC1 null CT43 line compared with the CHO wild-type line (flotillin-2-GFP increase to 278%, S.E. = 23%, $n = 9$, $p = 0.0004$, Mann-Whitney *U* test and cholesterol increase to 174%, S.E. = 15%, $n = 6$, $p = 0.002165$, Mann-Whitney *U* test). To test whether wild-type NPC1 could reverse the up-regulation of exosome secretion observed in the NPC1 null CT43 line, we transiently co-transfected cells with flotillin-2-GFP and either wild-type or mutant NPC1 and measured exosomal release of flotillin-2-GFP. The co-transfection approach with flotillin-2-GFP ensured that only exosomes were measured that originated from NPC1-transfected cells. As shown in Fig. 6*D*, co-transfection of flotillin-2-GFP and wild-type NPC1 into CT43 CHO cells reduced the amount of secreted flotillin-2-GFP-positive exosomes to the level released by flotillin-2-GFP-transfected wild-type CHO cells (107% as compared with wild-type CHO with 100%, S.E. = 24%, $n = 14$, $p = 1$, Mann-Whitney *U* test). Co-transfection of CT43 cells with flotillin-2-GFP and NPC1 bearing the P692S point mutation led to a reduction of exosome release compared with CT43 control cells transfected with flotillin-2-GFP only (28% reduction as compared with control CT43 cells, S.E. = 45%, $n = 14$, $p = 0.041$, Mann-Whitney *U* test). Exosome release was still higher than that from CT43 cells transfected with NPC1 wild-type or CHO wild-type cells, reflecting the reduced protein function of NPC1 P692S (99% increase compared with wild-type NPC1-transfected CT43 cells, $p = 0.047$, Mann-Whitney *U* test and 106% increase compared with CHO wild-type cells, $p = 0.13$, Mann-Whitney *U* test). The weak effect of NPC1 P692S transfection on exosome release most likely reflects the protein residual function (41). Transfection rates of NPC1 wild-type and NPC1 mutant were similar, as shown in supplemental Fig. S6*B*, ruling out different levels of NPC1 protein as the reason for the observed effects. In summary, these findings show that wild-type NPC1 can reverse the enhanced exosome secretion observed under NPC1 null conditions, whereas NPC1 carrying the point mutation P692S within its sterol-sensing domain was described to have reduced function and could not fully reverse the NPC1 null related increase in exosome release (41). Transfection of the NPC1 point mutant into CT43 cells reflects the compound heterozygous mutation in the patient fibroblasts that results in NPC1 truncation (R934*X*) and reduced NPC1 activity due to the P1007A point mutation (42).

DISCUSSION

The aim of this study was to determine whether exosomes have a function in cellular cholesterol homeostasis. In summary, we have shown that free cholesterol can be released by exosomes, a process that is dependent on flotillin. Exosomal cholesterol release is up-regulated under conditions of cholesterol oversupply and in NPC1 disease, where it might serve as a mechanism of the cell to partially overcome the presumably

cytotoxic accumulation of free cholesterol within late endosomes/lysosomes. Altogether our data hint toward a novel role for exosomes and flotillin in the regulation of cellular cholesterol homeostasis.

Loading the cell with free cholesterol increases the endosomal pool of flotillin. Similar to our findings, Langhorst *et al.* (43) observed a cholesterol-dependent intracellular distribution of flotillin in HeLa cells. Challenging the cell with cholesterol enhances both the exosomal release of flotillin-2 and cholesterol. The exosomal secretion of cholesterol depends on the presence of flotillin-2 and on cholesterol-interacting CRAC domains within the flotillin-2 molecule. Supporting our data, it was recently reported that EGF-mediated endocytosis and sorting of flotillin-2 into CD63-positive endosomes was impaired by the Y163F mutation in the second CRAC domain of flotillin-2 (44). Down-stream signaling of EGF involves the activation of src kinases, and the authors, therefore, speculated that the reduction of flotillin-2 Y163F endocytosis might be due to the absent tyrosine phosphorylation site Tyr-163. However, we did not detect a difference in the distribution of flotillin-2 between plasma membrane and endocytic pools after inhibition of src kinases by PP-2 in oligodendroglial cells. The finding that exosomal release of cholesterol is hampered by flotillin knockdown further hints toward a function of flotillin in recruiting cholesterol to MVBs and exosomes.

Increasing levels of free cholesterol not only promote flotillin endocytosis but also enhance the amount of exosome secretion, whereas metabolic cholesterol depletion by simvastatin decreases the release of flotillin-positive exosomes. Based on these data alone, it is difficult to discriminate between an enrichment of cholesterol in a single exosome particle and an up-regulation of the absolute number of secreted exosomes. Both mechanisms would result in efflux of trapped cholesterol from the cell. However, the cholesterol-induced increase of several marker proteins (flotillin-2, alix, EGFP-CD63, PLP-myc) within the exosomal fraction favors the notion of an up-regulated vesicle release.

Recently, the increased exosomal release of the latent membrane protein 2A of Epstein-Barr virus was reported upon mβCD-mediated cholesterol depletion (45). Our data indicate that different subsets of exosomes are released by distinct regulatory mechanisms, as shown by the cholesterol-independent release of Gag-positive endosomes, which bud directly from the plasma membrane. In contrast, the release of flotillin-2-positive exosomes is enhanced by high cholesterol levels. We propose that these exosomes derive from the indirect MVB-dependent pathway, as the flotillin CRAC mutant, which is severely impaired in endocytosis from the plasma membrane, is not released via exosomes in response to cholesterol treatment.

siRNA-mediated knockdown of flotillin-2 reduces exosomal cholesterol release. The amount of cholesterol within the cell is tightly regulated by equilibrium between synthesis, uptake from the extracellular space, and efflux of cholesterol from the cell. An active transport of free cholesterol from the cell relies on cholesterol transporter proteins. Here we provide evidence for an additional, flotillin-dependent exosome pathway, by which free cholesterol can leave the cell. Cholesterol accumulates within the endocytic pathway in intraluminal vesicles of MVBs, and up to 63% of the endocytic cholesterol localizes to this compartment (17, 46). Exosomes do not only differ in their protein composition but also in their lipid content, which varies depending on their cellular origin (47). Mast cells, like dendritic cells and reticulocytes, release exosomes with similar proportions of cholesterol and phospholipids as the parent cell membranes (48, 49). In contrast, B and T lymphocyte-derived exosomes are enriched in cholesterol (9, 50). Our data indicate that free cholesterol is partially released by exosomes, a pathway that is up-regulated in response to increased levels of free cholesterol in late endosomal/lysosomal compartments. Strikingly, null mutants of the *Drosophila* NPC1a show neuronal cholesterol accumulation followed by the appearance of multivesicular organelles, and accumulation of multivesicular profiles was also found in brains of NPC1$^{-/-}$ mice (51, 52). Exocytosis of storage material has been reported previously in cultured primary kidney cells derived from arylsulfatase A-deficient mice, an animal model for the lysosomal storage disease metachromatic leukodystrophy (53). In addition to cholesterol, also marked sphingolipid accumulation is observed within late endosomes in NPC type 1. The question of whether sphingolipid release by exosomes is up-regulated in a similar fashion as cholesterol and whether the overall lipid composition of NPC1 exosomes is altered awaits further analysis. In addition, further research is needed to study the significance of exosome secretion *in vivo*, *e.g.* in NPC1$^{-/-}$ mice and mouse models of other endosomal storage diseases. In summary, we provided evidence that the enhanced rate of exosomal cholesterol release might serve as a mechanism to eliminate excessively accumulated cholesterol in the late endosomal/lysosomal compartments in the lipid storage disease NPC. Our finding is especially interesting in light of the unexpectedly low brain concentrations of cholesterol in late disease stages of NPC, a fact that seems counterintuitive at first sight (54). Low axonal cholesterol levels might reflect the enhanced exosomal secretion of cholesterol in NPC and are consistent with the loss of function hypothesis in NPC, which explains the pathomechanism of the disease by a shortage of axonal plasma membrane cholesterol despite intracellular cholesterol accumulation (55–57).

Cholesterol fulfils an important function in maintaining membrane properties such as thickness and fluidity, which is necessary for proper neuronal function. Furthermore, the up-regulation of exosome production in the cerebrospinal fluid opens new perspectives regarding cerebrospinal fluid biomarkers of NPC disease activity. The lack of availability of such markers has hampered the validation of pharmaceutical compounds on disease progression. The quantitative determination of exosomes in NPC cerebrospinal fluid might, therefore, be an interesting candidate for the development of longitudinal biomarkers.

REFERENCES

1. van Niel, G., Porto-Carreiro, I., Simoes, S., and Raposo, G. (2006) *J. Biochem.* **140,** 13–21
2. Keller, S., Sanderson, M. P., Stoeck, A., and Altevogt, P. (2006) *Immunol. Lett.* **107,** 102–108
3. Belting, M., and Wittrup, A. (2008) *J. Cell Biol.* **183,** 1187–1191
4. Simons, M., and Raposo, G. (2009) *Curr. Opin Cell Biol.* **21,** 575–581
5. Montecalvo, A., Shufesky, W. J., Stolz, D. B., Sullivan, M. G., Wang, Z.,

Divito, S. J., Papworth, G. D., Watkins, S. C., Robbins, P. D., Larregina, A. T., and Morelli, A. E. (2008) *J. Immunol.* **180,** 3081–3090
6. Valadi, H., Ekström, K., Bossios, A., Sjöstrand, M., Lee, J. J., and Lötvall, J. O. (2007) *Nat. Cell Biol.* **9,** 654–659
7. Fauré, J., Lachenal, G., Court, M., Hirrlinger, J., Chatellard-Causse, C., Blot, B., Grange, J., Schoehn, G., Goldberg, Y., Boyer, V., Kirchhoff, F., Raposo, G., Garin, J., and Sadoul, R. (2006) *Mol. Cell Neurosci.* **31,** 642–648
8. Johnstone, R. M., Mathew, A., Mason, A. B., and Teng, K. (1991) *J. Cell. Physiol.* **147,** 27–36
9. Wubbolts, R., Leckie, R. S., Veenhuizen, P. T., Schwarzmann, G., Möbius, W., Hoernschemeyer, J., Slot, J. W., Geuze, H. J., and Stoorvogel, W. (2003) *J. Biol. Chem.* **278,** 10963–10972
10. Vance, J. E., Hayashi, H., and Karten, B. (2005) *Semin. Cell Dev. Biol.* **16,** 193–212
11. Chang, T. Y., Chang, C. C., Ohgami, N., and Yamauchi, Y. (2006) *Annu. Rev. Cell Dev. Biol.* **22,** 129–157
12. Infante, R. E., Wang, M. L., Radhakrishnan, A., Kwon, H. J., Brown, M. S., and Goldstein, J. L. (2008) *Proc. Natl. Acad. Sci. U.S.A.* **105,** 15287–15292
13. Liscum, L., and Sturley, S. L. (2004) *Biochim. Biophys. Acta* **1685,** 22–27
14. Chang, T. Y., Reid, P. C., Sugii, S., Ohgami, N., Cruz, J. C., and Chang, C. C. (2005) *J. Biol. Chem.* **280,** 20917–20920
15. Vanier, M. T., Rodriguez-Lafrasse, C., Rousson, R., Gazzah, N., Juge, M. C., Pentchev, P. G., Revol, A., and Louisot, P. (1991) *Biochim. Biophys. Acta* **1096,** 328–337
16. Sturley, S. L., Patterson, M. C., Balch, W., and Liscum, L. (2004) *Biochim. Biophys. Acta* **1685,** 83–87
17. Fitzner, D., Schneider, A., Kippert, A., Möbius, W., Willig, K. I., Hell, S. W., Bunt, G., Gaus, K., and Simons, M. (2006) *EMBO J.* **25,** 5037–5048
18. Bartz, F., Kern, L., Erz, D., Zhu, M., Gilbert, D., Meinhof, T., Wirkner, U., Erfle, H., Muckenthaler, M., Pepperkok, R., and Runz, H. (2009) *Cell Metab.* **10,** 63–75
19. Cruz, J. C., Sugii, S., Yu, C., and Chang, T. Y. (2000) *J. Biol. Chem.* **275,** 4013–4021
20. Trajkovic, K., Dhaunchak, A. S., Goncalves, J. T., Wenzel, D., Schneider, A., Bunt, G., Nave, K. A., and Simons, M. (2006) *J. Cell Biol.* **172,** 937–948
21. Schneider, A., Rajendran, L., Honsho, M., Gralle, M., Donnert, G., Wouters, F., Hell, S. W., and Simons, M. (2008) *J. Neurosci.* **28,** 2874–2882
22. Trajkovic, K., Hsu, C., Chiantia, S., Rajendran, L., Wenzel, D., Wieland, F., Schwille, P., Brügger, B., and Simons, M. (2008) *Science* **319,** 1244–1247
23. Bauer, M., and Pelkmans, L. (2006) *FEBS Lett.* **580,** 5559–5564
24. Langhorst, M. F., Reuter, A., and Stuermer, C. A. (2005) *Cell. Mol. Life Sci.* **62,** 2228–2240
25. Kokubo, H., Helms, J. B., Ohno-Iwashita, Y., Shimada, Y., Horikoshi, Y., and Yamaguchi, H. (2003) *Brain Res.* **965,** 83–90
26. Roitbak, T., Surviladze, Z., Tikkanen, R., and Wandinger-Ness, A. (2005) *Biochem. J.* **392,** 29–38
27. Glebov, O. O., Bright, N. A., and Nichols, B. J. (2006) *Nat. Cell Biol.* **8,** 46–54
28. Fassbender, K., Simons, M., Bergmann, C., Stroick, M., Lutjohann, D., Keller, P., Runz, H., Kuhl, S., Bertsch, T., von Bergmann, K., Hennerici, M., Beyreuther, K., and Hartmann, T. (2001) *Proc. Natl. Acad. Sci. U.S.A.* **98,** 5856–5861
29. Li, H., Yao, Z., Degenhardt, B., Teper, G., and Papadopoulos, V. (2001) *Proc. Natl. Acad. Sci. U.S.A.* **98,** 1267–1272
30. Jamin, N., Neumann, J. M., Ostuni, M. A., Vu, T. K., Yao, Z. X., Murail, S., Robert, J. C., Giatzakis, C., Papadopoulos, V., and Lacapère, J. J. (2005) *Mol. Endocrinol.* **19,** 588–594
31. Fang, Y., Wu, N., Gan, X., Yan, W., Morrell, J. C., and Gould, S. J. (2007) *PLoS Biol.* **5,** e158
32. Solis, G. P., Hoegg, M., Munderloh, C., Schrock, Y., Malaga-Trillo, E., Rivera-Milla, E., and Stuermer, C. A. (2007) *Biochem. J.* **403,** 313–322
33. Koh, C. H., and Cheung, N. S. (2006) *Cell. Signal.* **18,** 1844–1853
34. Chang, T. Y., Chang, C. C., Bryleva, E., Rogers, M. A., and Murphy, S. R. (2010) *IUBMB Life* **62,** 261–267
35. Infante, R. E., Wang, M. L., Radhakrishnan, A., Kwon, H. J., Brown, M. S., and Goldstein, J. L. (2008) *Proc. Natl. Acad. Sci. U.S.A.* **7,** 15287–15292
36. Infante, R. E., Abi-Mosleh, L., Radhakrishnan, A., Dale, J. D., Brown, M. S., and Goldstein, J. L. (2008) *J. Biol. Chem.* **283,** 1052–1063
37. Infante, R. E., Radhakrishnan, A., Abi-Mosleh, L., Kinch, L. N., Wang, M. L., Grishin, N. V., Goldstein, J. L., and Brown, M. S. (2008) *J. Biol. Chem.* **283,** 1064–1075
38. Kwon, H. J., Abi-Mosleh, L., Wang, M. L., Deisenhofer, J., Goldstein, J. L., Brown, M. S., and Infante, R. E. (2009) *Cell* **137,** 1213–1224
39. Deleted in proof
40. Hua, X., Nohturfft, A., Goldstein, J. L., and Brown, M. S. (1996) *Cell* **87,** 415–426
41. Millard, E. E., Gale, S. E., Dudley, N., Zhang, J., Schaffer, J. E., and Ory, D. S. (2005) *J. Biol. Chem.* **280,** 28581–28590
42. Bauer, S. H., Wiechers, M. F., Bruns, K., Przybylski, M., and Stuermer, C. A. (2001) *Anal. Biochem.* **298,** 25–31
43. Langhorst, M. F., Reuter, A., Jaeger, F. A., Wippich, F. M., Luxenhofer, G., Plattner, H., and Stuermer, C. A. (2008) *Eur. J. Cell Biol.* **87,** 211–226
44. Neumann-Giesen, C., Fernow, I., Amaddii, M., and Tikkanen, R. (2007) *J. Cell Sci.* **120,** 395–406
45. Matsuzaki, K., Noguch, T., Wakabayashi, M., Ikeda, K., Okada, T., Ohashi, Y., Hoshino, M., and Naiki, H. (2007) *Biochim. Biophys. Acta* **1768,** 122–130
46. Kolter, T., and Sandhoff, K. (2005) *Annu. Rev. Cell Dev. Biol.* **21,** 81–103
47. Subra, C., Laulagnier, K., Perret, B., and Record, M. (2007) *Biochimie* **89,** 205–212
48. Vidal, M., Sainte-Marie, J., Philippot, J. R., and Bienvenue, A. (1989) *J. Cell. Physiol.* **140,** 455–462
49. Laulagnier, K., Motta, C., Hamdi, S., Roy, S., Fauvelle, F., Pageaux, J. F., Kobayashi, T., Salles, J. P., Perret, B., Bonnerot, C., and Record, M. (2004) *Biochem. J.* **380,** 161–171
50. Zakharova, L., Svetlova, M., and Fomina, A. F. (2007) *J. Cell. Physiol.* **212,** 174–181
51. Phillips, S. E., Woodruff, E. A., 3rd, Liang, P., Patten, M., and Broadie, K. (2008) *J. Neurosci.* **28,** 6569–6582
52. Liao, G., Yao, Y., Liu, J., Yu, Z., Cheung, S., Xie, A., Liang, X., and Bi, X. (2007) *Am. J. Pathol.* **171,** 962–975
53. Klein, D., Büssow, H., Fewou, S. N., and Gieselmann, V. (2005) *Biochem. Biophys. Res. Commun.* **327,** 663–667
54. Xie, C., Burns, D. K., Turley, S. D., and Dietschy, J. M. (2000) *J. Neuropathol. Exp. Neurol.* **59,** 1106–1117
55. Karten, B., Vance, D. E., Campenot, R. B., and Vance, J. E. (2002) *J. Neurochem.* **83,** 1154–1163
56. Karten, B., Vance, D. E., Campenot, R. B., and Vance, J. E. (2003) *J. Biol. Chem.* **278,** 4168–4175
57. Tashiro, Y., Yamazaki, T., Shimada, Y., Ohno-Iwashita, Y., and Okamoto, K. (2004) *Eur. J. Neurosci.* **20,** 2015–2021